ACS OMEGA

http://pubs.acs.org/journal/acsodf

Article

High Blocking Capacity of Fuzzy-Ball Fluid to Further Enhance Oil Recovery after Polymer Flooding in Heterogeneous Sandstone Reservoirs

Chao Wang,* Hao Liu, Xiangchun Wang, and Lihui Zheng*

Cite This: *ACS Omega* 2021, 6, 34035−34043

Read Online

ACCESS | Metrics & More | Article Recommendations

ABSTRACT: Even after a long time of polymer flooding, over half of the crude oil is still trapped in the reservoir due to the poor plugging capacity. It has been demonstrated that fuzzy-ball fluid can be utilized as an effective plugging fluid. The idea of further increasing oil recovery by fuzzy-ball fluid following polymer flooding drew us to investigate it due to its high performance and effect. In this paper, seepage behavior experiments and parallel core displacement experiments were carried out to evaluate the plugging ability and oil displacement effect of fuzzy-ball fluid. Also, the microscopic blocking mechanism of fuzzy-ball fluid was observed. The results showed that fuzzy-ball fluid has a good plugging capability thanks to the pressure consumption and accumulation plugging mechanisms. The resistance coefficient and residual resistance coefficient of fuzzy-ball fluid are also substantially greater than those of the polymer, at 76.25−239.96 and 13.95−49.91, respectively. Due to its outstanding plugging capability, fuzzy-ball fluid can achieve complete fluid diversion, with the flow fraction of the high-permeability core reduced to nearly 0% and that of the low-permeability core increased to nearly 100%. As a result, low-permeability core oil recovery and total oil recovery both can be enhanced by 46.12−49.24 and 22.81−24.40%, respectively. A field test of fuzzy-ball fluid flooding was carried out in wells TX_1 and TX_2 which have been flooding with polymers. After the fuzzy-ball fluid was introduced, total daily oil production increased by 64.15%. Fuzzy-ball fluid can significantly boost oil recovery after polymer flooding, according to laboratory and field trials, providing a technical solution for heterogeneous sandstone reservoirs to further enhance oil recovery.

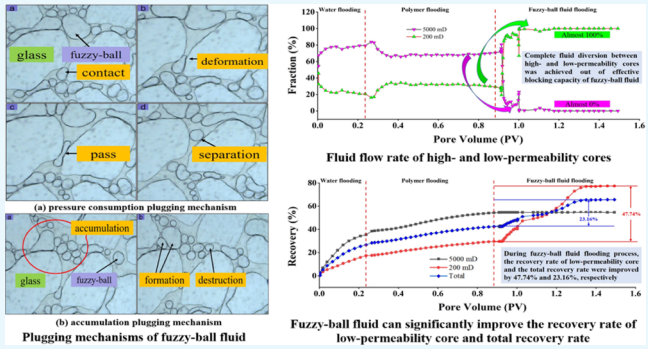

1. INTRODUCTION

Since being discovered and utilized, petroleum resources have been playing a significant role in every aspect of people's daily life and social development. According to the BP Statistical Review of World Energy 2020, total oil consumption in 2019 was 193EJ, accounting for 33.05% of total energy consumption. As a result, scientists and oil workers have been working tirelessly to extract oil from the ground. However, due to significant formation heterogeneity, oil recovery is severely limited, particularly in relatively low-permeability areas.

In the last few decades, various methods[1−6] have been used to improve oil recovery. Polymer flooding is one of the most widely used of these techniques. Polymers[7,8] can reduce the oil−water mobility ratio and increase the sweeping volume which lead to improved oil recovery out of its viscosity. Nowadays, polymers have been widely industrially used in many oil fields and have achieved certain results.[9−11] However, polymers have limited viscosity, which limits their ability to increase the sweeping volume.[12,13] Simultaneously, polymers have poor shear resistance,[14] salinity resistance,[15] and temperature resistance,[16] and viscosity was reduced further after injection into the reservoir. Furthermore, after water flooding, the reservoir will form a dominant channel for water flow, which will change the pore structure of the reservoir.[17,18] All of these factors contribute to polymers' limited ability to plug dominant channels and increase sweeping volume. Therefore, polymers can only increase oil recovery by about 10%, and approximately 50% of the geological reserves still remain trapped after polymer flooding.[19,20]

After extensive research and testing, Zheng et al. developed fuzzy-ball fluid[21] in 2010. Fuzzy-ball fluid is a two-phase fluid composed of a fluid and fuzzy-ball. The fuzzy-ball structure (Figure 1b) is a bionic structure that is similar to the structure

Received: September 30, 2021
Accepted: November 24, 2021
Published: December 3, 2021

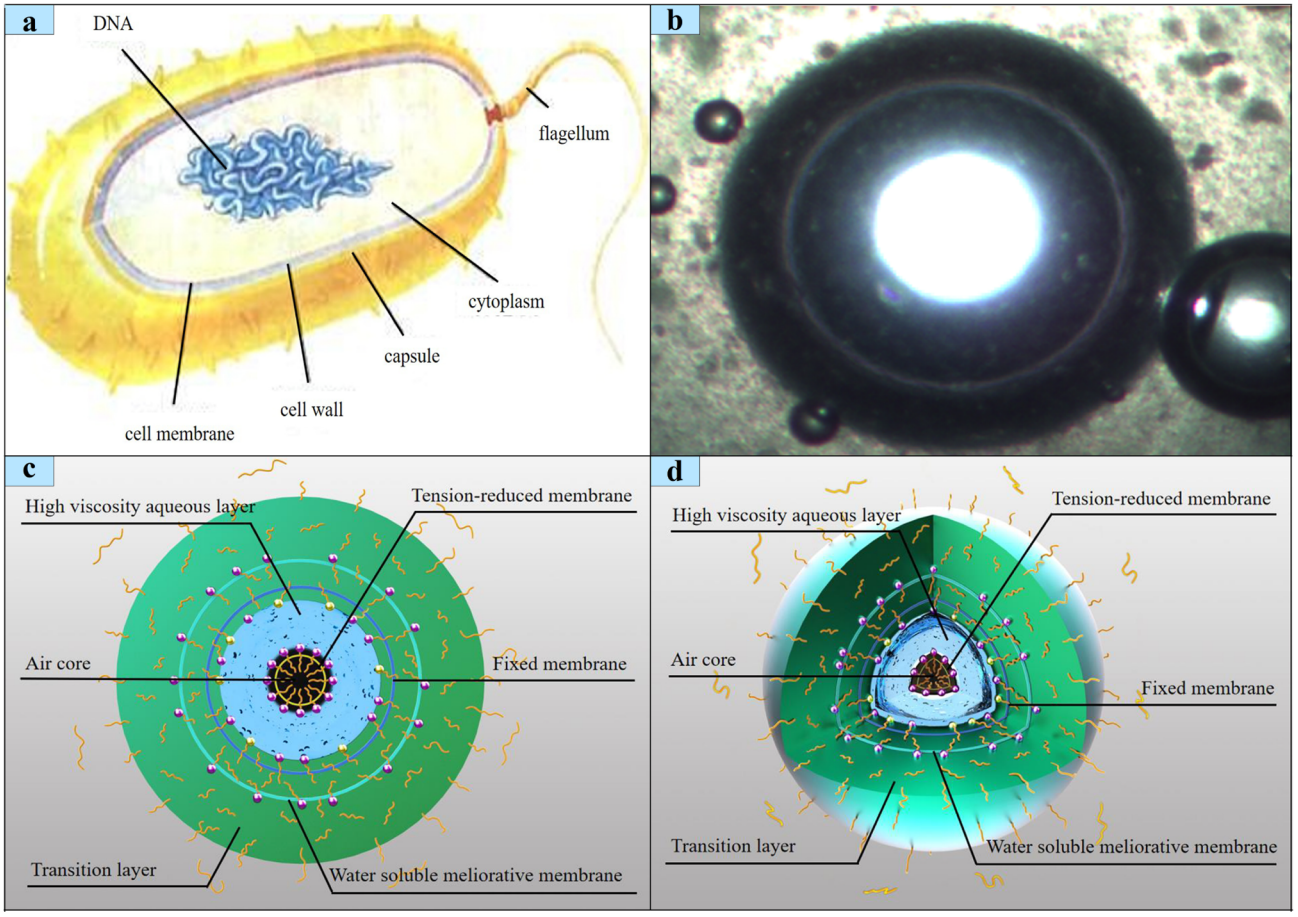

Figure 1. Structure of bacteria and a fuzzy ball. (a) Bacteria; (b) fuzzy ball of 400× under an optical microscope; (c) planar diagram of a fuzzy ball, and (d) space diagram of a fuzzy ball.

of bacteria (Figure 1a[22]). One air core, two layers (high viscosity aqueous layer and transition layer), and three membranes (tension-reduce membrane, fixed membrane, and water soluble meliorative membrane) comprise the fuzzy-ball (Figure 1c,d). Fuzzy-ball has a variety of characteristics due to its unique structure. First and foremost, due to its two-layer and three-membrane structure, fuzzy-ball has high stability and can withstand high pressure and mechanical shear. Furthermore, because of the presence of the gas core, fuzzy-ball has a high deformability and can be used to plug core pores of various sizes. As a result, when compared to polymers, gels, and polymer microspheres, fuzzy-ball fluid has superior blocking ability and has gained a wide range of on-field applications, including drilling,[23,24] workover,[25] oil stabilizing and water controlling,[26] and fracturing.[27,28] However, there has been little research and application of fuzzy-ball fluid in the enhancement of oil recovery.

Wei et al.[29] investigated the oil displacement effect of fuzzy-ball fluid in 2020. According to the results of the experiments, fuzzy-ball fluid can improve oil recovery by approximately 20% after water flooding, indicating that fuzzy-ball is feasible for oil displacement. The main focus of the research, however, is on the extraction capacity of fuzzy-ball fluid as a displacement agent following water flooding. The displacement effect of fuzzy-ball fluid following polymer flooding has not been investigated further. Furthermore, the plugging mechanism of fuzzy-ball fluid in improving oil recovery is not discussed.

In this paper, displacement effect of fuzzy-ball fluid after polymer flooding in sandstone reservoirs was investigated and the plugging mechanism of fuzzy-ball fluid was measured and analyzed. First, the microstructure of fuzzy-ball was examined. In addition, the matching relationship between the fuzzy-ball and the pore aperture of cores was investigated. Then, seepage behavior and parallel core displacement experiments were performed. Furthermore, the microscopic blocking mechanism of fuzzy-ball fluid was investigated. Finally, the fuzzy-ball fluid field test results were examined.

2. RESULTS AND DISCUSSION

2.1. Injection Performance of Fuzzy-Ball Fluid. Using the pressure curve of the core with a gas permeability of 5000 mD as an example, Figure 2 shows that the maximum injection pressure of fuzzy-ball fluid can reach more than 13 MPa and subsequent water flooding injection pressure can reach more than 2 MPa. The pressure curve exhibits a fluctuating characteristic of "increase−decrease−increase−decrease−..." during and after the injection process of fuzzy-ball fluid. This is related to the fuzzy-ball fluid plugging mechanism, which will be discussed in detail in Section 2.3.

Because the injection pressure of fuzzy-ball fluid is constantly changing during the injection process, conventional formulas cannot be used to calculate the resistance coefficient and residual resistance coefficient of fuzzy-ball fluid. As a result, in order to characterize the sealing ability of fuzzy-ball fluid during the injection process, the maximum resistance

https://doi.org/10.1021/acsomega.1c05427
ACS Omega 2021, 6, 34035−34043

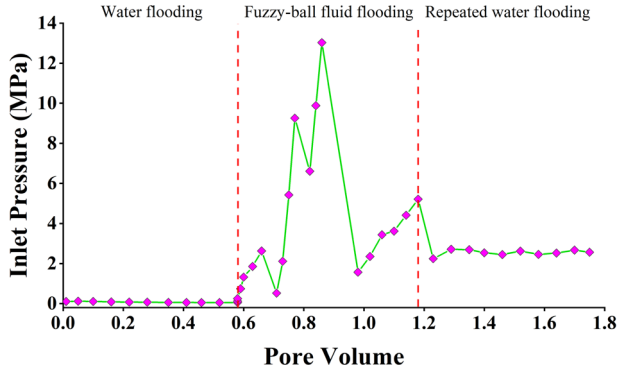

Figure 2. Pressure curve of water flooding, fuzzy-ball fluid flooding, and repeated water flooding.

coefficient (F_{MR}) and maximum residual resistance coefficient (F_{MRR}) are defined as follows

$$F_{MR} = \frac{K_w}{\mu_w} \times \frac{\mu_f}{K_f} \quad (1)$$

$$F_{MRR} = \frac{K_w'}{K_w} \quad (2)$$

where K_w, K_f, and K_w' are permeabilities during the injection process of simulated formation water, fuzzy-ball fluid, and repeated simulated formation water, respectively. μ_w and μ_f are viscosities of simulated formation water and fuzzy-ball fluid, respectively.

Figure 3 depicts the F_{MR} and F_{MRR} of fuzzy-ball fluid in cores with a gas permeability of 200, 600, 1200, and 5000 mD.

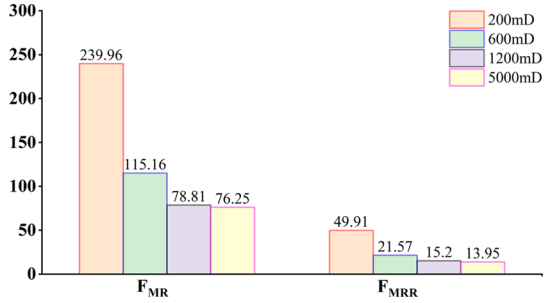

Figure 3. F_{MR} and F_{MRR} of fuzzy-ball fluid in different cores.

As shown in Figure 3, the F_{MR} of 200, 600, 1200, and 5000 mD is 76.25, 78.81, 115.16, and 239.96, respectively, and the F_{MRR} is 13.95, 15.20, 21.57, and 49.91, respectively. The F_{MR} and F_{MRR} of fuzzy-ball fluid are significantly greater than those of polymers[30] and gels,[31] which are commonly used in profile control and enhanced oil recovery (EOR). It demonstrates that fuzzy-ball fluid has excellent sealing property and has a high potential for further EOR after polymer displacement.

2.2. Effect of Fuzzy-Ball Fluid to Improve Oil Recovery after Polymer Flooding. The curves in Figure 4 illustrate the fluid flow rate, inlet pressure, and oil recovery during the injection process using cores with a gas permeability of 200 and 5000 mD. The injected polymer preferentially enters the high-permeability core during the polymer flooding process. As the polymer accumulates, the flow resistance of the high-permeability core increases due to the polymer's specific viscosity, allowing the subsequent polymer to enter the low-permeability core more easily. As a result, the high-permeability core's flow rate decreased, while the low-permeability core's flow rate increased. This results in an increase in recovery of both the high- and low-permeability cores. However, due to the polymer's limited plugging effect, as indicated by the small increase in polymer injection pressure, the recovery rate of the high-permeability and low-permeability cores increased by only 19.03 and 12.18%, respectively, while the total recovery rate increased by 15.72%.

During the injection process, fuzzy-ball fluid preferentially enters the hyperpermeable core, accumulates in the high-permeability core's seepage channels, and blocks the high-permeability core's seepage channels. The fluid flow begins to divert and flow into the low-permeability core as the fuzzy-ball fluid seals the high-permeability core. The flow rate of the high-permeability core and the low-permeability core is equal after injecting about 0.05 pore volume (PV) of fuzzy-ball fluid. As the injection continued, the flow rate of the low-permeability core gradually increased above 90%, while that of the high-permeability core gradually decreased less than 10%, indicating complete fluid diversion. This shows that the high-permeability core's seepage channels have been almost completely blocked, which is also supported by the fact that the inlet pressure has been kept above 4 MPa. Simultaneously, the sweeping volume of the low-permeability core increased significantly. As a result, the recovery rate of the low-permeability and high-permeability cores were improved by 47.74 and 0.26%, respectively. Furthermore, the overall recovery rate was increased by 23.16%. Figure 5 depicts the recovery of different groups in parallel core displacement experiments.

As illustrated in Figure 5, the recovery rate of low-permeability cores and total recovery rate can be enhanced by 46.12−49.24 and 22.81−24.40%, respectively, during the process of fuzzy-ball fluid flooding. However, the recovery rate of high-permeability cores was increased by just 0.26−0.52%. The results indicate that fuzzy-ball fluid can significantly improve the rate of recovery of low-permeability cores and the overall rate of recovery following polymer flooding. However, it has minimal effect on increasing the recovery rate of cores with a high permeability.

2.3. Plugging Mechanism of Fuzzy-Ball Fluid. As previously stated, fuzzy-ball fluid's outstanding blocking ability enables it to significantly boost oil recovery following polymer flooding. As a result, the reasons for fuzzy-ball fluid's superior plugging ability must be examined.

2.3.1. Relationships between Fuzzy-Ball Size and Pore Diameter of Core Samples. The size distribution of fuzzy balls (Figure 6a) and the pore diameter of core samples with varying permeabilities (Figure 6b) were characterized in order to investigate their matching relationships. The diameter of 300 fuzzy balls was measured using an optical microscope, and the pore size of core samples was determined using a Micromeritics Auto Pore IV 9500.

The size distribution range of the fuzzy-balls is 0−500 μm, as shown in Figure 6a. Furthermore, the size of the fuzzy ball is primarily distributed in the range of 100−200 μm, with the proportion of that being close to 50%. The pore size distribution range of four core samples is 0−100 μm in Figure 6b, and the maximum pore diameters of core samples with 200, 600, 1200, and 5000 mD are 7.24, 13.94, 21.31, and 30.17 μm, respectively. The relationship between fuzzy-ball size and pore diameter can be divided into two categories based on

https://doi.org/10.1021/acsomega.1c05427
ACS Omega 2021, 6, 34035−34043

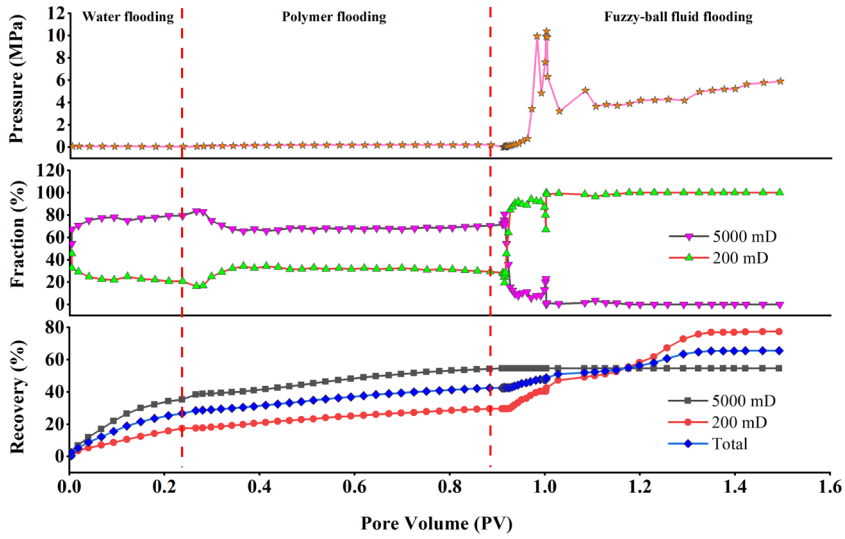

Figure 4. Curves of fraction, inlet pressure, and recovery of cores (200and 5000 mD) in parallel core displacement experiments.

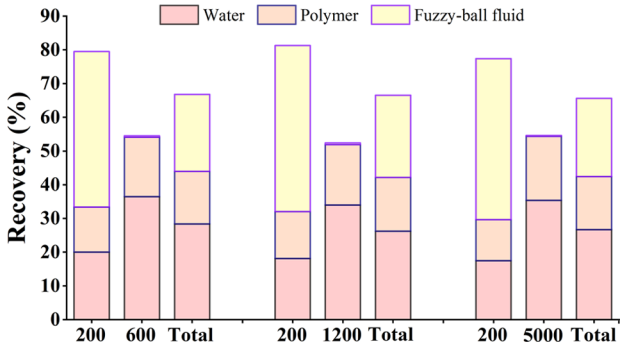

Figure 5. Recovery of different groups in parallel core displacement experiments.

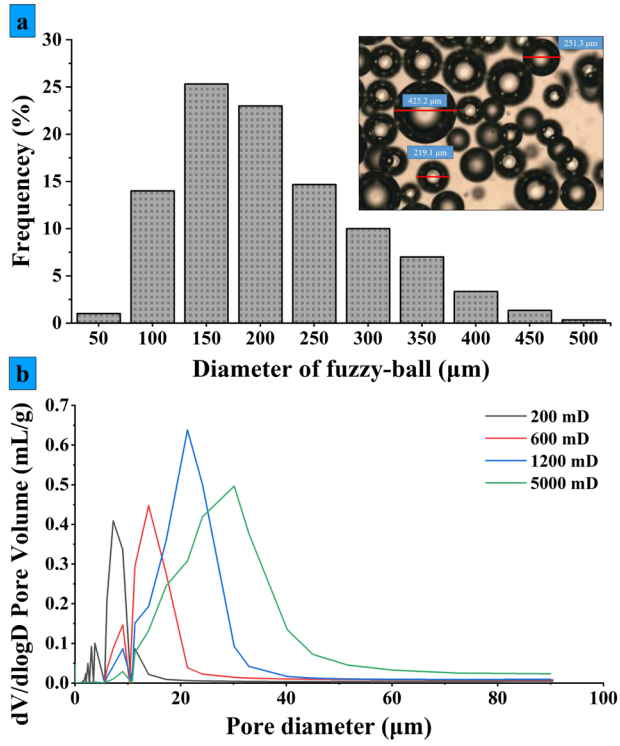

Figure 6. Size distribution of fuzzy balls (a) and pore diameter distribution of core samples (b).

their size distribution ranges: (a) the size of the fuzzy ball is greater than or equal to the pore diameter and (b) the size of the fuzzy ball is smaller than the pore diameter. As a result, there are two mechanisms for the fuzzy-ball fluid to seal core pores. Furthermore, because the main size distribution of the fuzzy ball is greater than the maximum diameter of the core pore, the first type of blocking mechanism predominates.

2.3.2. Pressure Consumption Plugging Mechanism. The plugging mechanism of fuzzy-ball fluid was studied using a microscopic glass etching model. As illustrated in Figure 7, when the size of the fuzzy ball is greater than or equal to the diameter of the pore, the fuzzy-ball seals the core pore through pressure consumption. The pressure consumption method can be divided into four steps: (a) contact. When the fuzzy-ball fluid is moved to the core pore, it begins to contact the core pore; (b) deformation. The fuzzy-ball begins to deform as a result of the injection pressure. The fuzzy ball can consume a portion of the injection pressure during the deformation process, causing the injection pressure to rise; (c) pass. The fuzzy ball is continuously compressed and deformed as a result of the continuous action of injection pressure. The fuzzy ball enters the core pore when it is deformed to match the diameter of the pore. On the one hand, maintaining the compression and deformation of the fuzzy ball in the process of passing through the core pore necessitates a certain amount of pressure; on the other hand, it necessitates a certain amount of pressure to overcome the frictional force between the surface of the fuzzy ball and the wall of the core pore. Both methods result in an increase in injection pressure. (d) Separation. After passing through the core pore, the fuzzy ball returns to its original shape and continues forward. The increase in injection pressure caused by a single fuzzy ball may be limited by a pressure-dissipating method. However, when there are a large number of fuzzy balls passing through the core pore, the injection pressure increase caused by the pressure consumption method will be significant.

2.3.3. Accumulation Plugging Mechanism. When the size of the fuzzy ball is smaller than the diameter of the core pore, the fuzzy-ball accumulates and plugs the core pore. Several fuzzy balls accumulate during the injection procedure to form

https://doi.org/10.1021/acsomega.1c05427
ACS Omega 2021, 6, 34035−34043

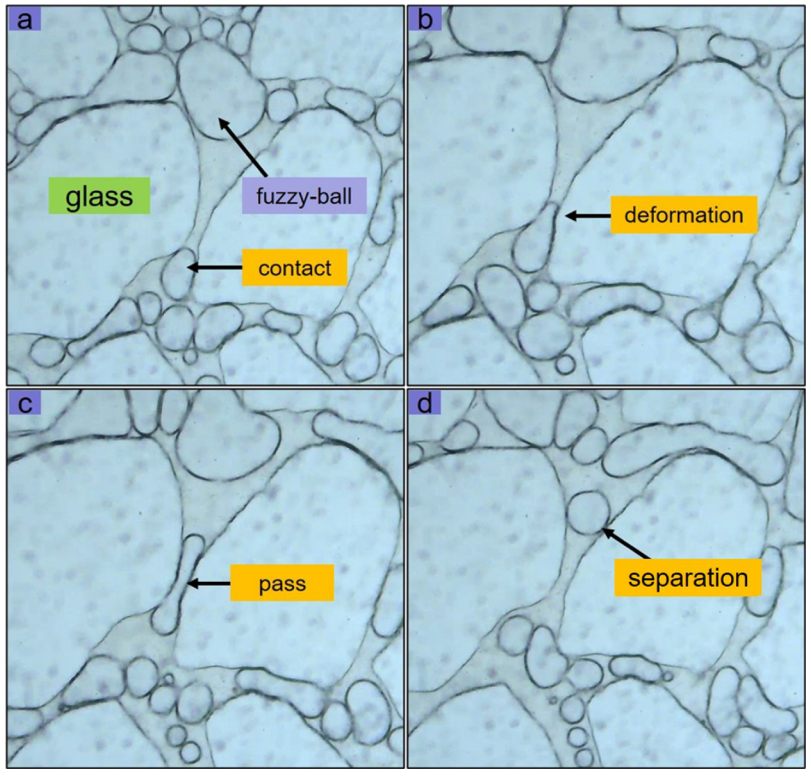

Figure 7. Schematic diagram of pressure consumption plugging mechanism of the fuzzy ball. (a) Contact; (b) deformation; (c) pass; and (d) separation.

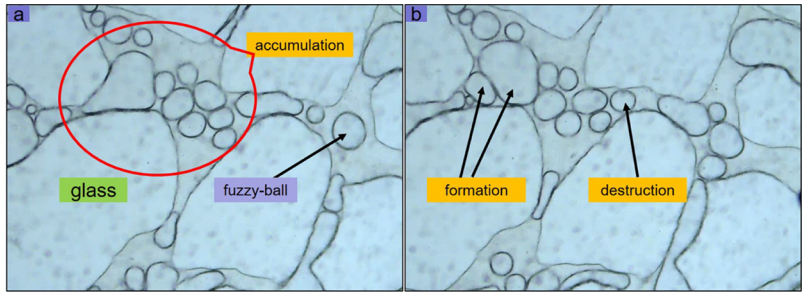

Figure 8. Schematic diagram of the accumulation plugging mechanism of the fuzzy ball. (a) Fuzzy-ball cluster and (b) formation and destruction of the fuzzy-ball fluid cluster.

"fuzzy-ball clusters", as illustrated in Figure 8. Following cluster formation, two factors are critical for blocking. On the one hand, fuzzy balls have a floss structure, which enables the floss of various fuzzy balls to be brought together, as illustrated in Figure 9. That is, intertwining the floss can increase the mutual force between fuzzy balls; on the other hand, because fuzzy-ball fluid is hydrophilic (contact angle between fuzzy-ball fluid and core slice was 20.99°, as shown in Figure 10), it will exert a strong force on the core surface, which is also highly hydrophilic due to long-term water and polymer flooding.

The accumulation plugging method is divided into two steps: (a) old cluster destruction. One or more fuzzy balls detach from the cluster as a result of the continuous action of injection pressure. In this process, a certain amount of injection pressure will be consumed due to the action of the two forces mentioned above, resulting in an increase in injection pressure. (b) A new cluster is formed. When a fuzzy ball leaves a cluster, other fuzzy balls enter to form new

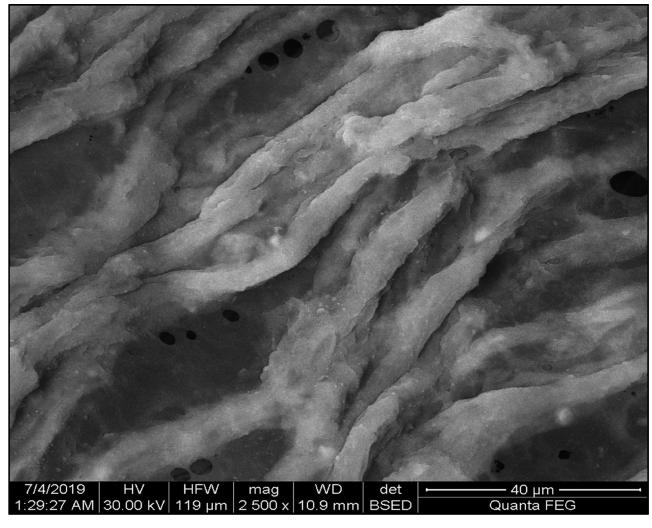

Figure 9. Floss of different fuzzy balls entwined together.

https://doi.org/10.1021/acsomega.1c05427
ACS Omega 2021, 6, 34035−34043

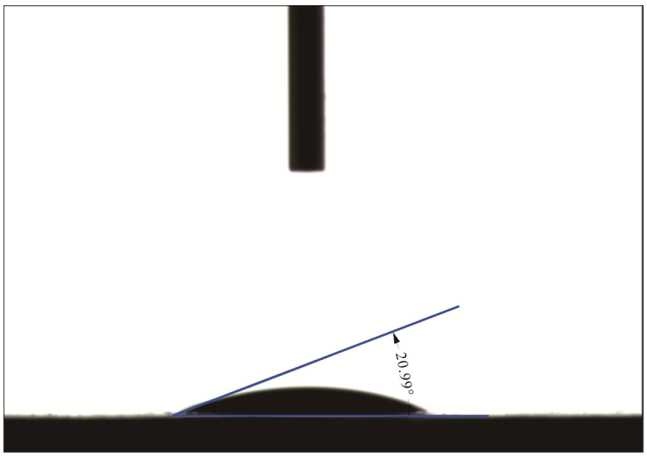

Figure 10. Surface tension of fuzzy-ball fluid on the core slice.

clusters. The two steps are continuously repeated, resulting in an increase in injection pressure.

3. FIELD TEST

A particular oil field in Northwest China is a typical conglomerate reservoir, with H_7 and H_6 sand formations running from bottom to top. The sedimentary thickness is 60−120 m, the sand thickness is 22.5 m on average, and the monolayer-sand conglomerate thickness is 35 m. With an average porosity of 18.7% and a permeability of 805.4 mD, the lithology is dominated by gravel-bearing coarse sandstone, small conglomerate, and sand conglomerate. Vertical multistage sand bodies are superimposed in the production area, with strong heterogeneity and interlayer and intralayer permeability ranges greater than 100, mud stone compartments are relatively thin, and plane distribution varies greatly.

The manufacturing area was developed in 1981, and water flooding began in 2013. Polymer injection began in September 2014. By June 2016, well TX_1 and well TX_2 were two injection wells in the region, corresponding to five oil wells with a total daily liquid production of 119.53 m^3/d and a total daily oil production of 9.01 m^3/d. Given that the region's inner layer is formed by water and polymer injection, the superior channel is clearly formed, while the inferior channel, which contains more oil, has a poor displacement effect. The effect of fuzzy-ball fluid regulation was tested in wells TX_1 and TX_2. In wells TX_1 and TX_2, 98 and 160 m^3 of fuzzy-ball fluid, respectively, were injected.

After 100 days of injection of fuzzy-ball fluid, total daily water production of five oil wells was 110.52 m^3/d and total daily production oil was 14.79 m^3/d. Compared with before the injection of fuzzy-ball fluid, total daily water production decreased by 13.23% and total daily oil production increased by 64.15%, as shown in Figure 11. All of the studies revealed that fuzzy-ball fluid can boost oil recovery even further following polymer flooding.

4. CONCLUSIONS

In this paper, seepage behavior experiments, parallel core displacement experiments, and field test were conducted. Additionally, the plugging mechanism of fuzzy-ball fluid was analyzed. The results indicate that:

Effective plugging capacity of fuzzy-ball fluid can be achieved through two kinds of mechanisms—"pressure consumption plugging mechanism" and "accumulation plugging mechanism". Additionally, seepage channel experiments show that the resistant coefficient and residual resistant coefficient of the fuzzy-ball fluid are much greater than those of polymers and gels.

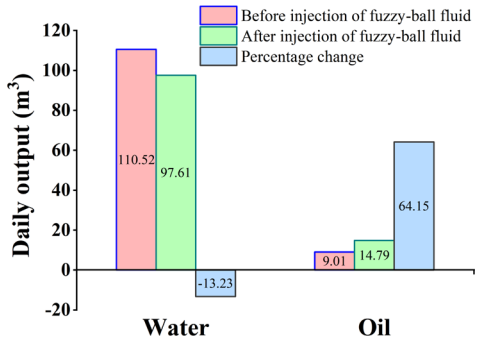

Figure 11. Daily water and oil production before and after injection of fuzzy-ball fluid.

After polymer flooding, fuzzy-ball fluid can further increase the recovery rate of low-permeability cores and total recovery rate by 46.12−49.24 and 22.81−24.40%, respectively. It indicates that fuzzy-ball fluid has great potential to be used to further enhance recovery after chemical recovery.

Although fuzzy-ball fluid can improve the recovery rate of low-permeability cores after polymer flooding, it can hardly improve that of high-permeability cores. Therefore, other displacement fluids can be used before fuzzy-ball fluid displacement to maximize the recovery rate of high-permeability cores.

5. EXPERIMENTAL MATERIALS AND METHODS

5.1. Experimental Materials. Fuzzy-ball coating, fuzzy-ball floss, fuzzy-ball core, and fuzzy-ball membrane agents were provided by Beijing Lihui Lab Energy Technology Co., Ltd., with a viscosity of 17.1 mPa·s at room temperature, and the polymer (3640C) used in the experiments was provided by China National Offshore Oil Corporation (CNOOC). Sodium chloride (NaCl), magnesium chloride ($MgCl_2$), sodium bicarbonate ($NaHCO_3$), and calcium chloride ($CaCl_2$) in the pure form were obtained from Sinopharm Group Co., Ltd. Artificial prismatic sandstone cores (45 mm × 45 mm × 300 mm) were provided by Beijing Jiade Yibang Petroleum Technology Development Co., Ltd. Water used in all experiments was deionized water.

5.2. Preparation of Samples. Simulated formation water: 1 g of NaCl, 0.1 g of $MgCl_2$, 0.4 g of $NaHCO_3$, and 0.2 g of $CaCl_2$ were blended using a blender with 1000 mL of deionized water for 20 min under a shearing rate of 1000 rpm and cooled to room temperature.

Polymer solution: 5 g of polymer powder was blended with 1000 mL of simulated formation water using a blender under a shearing rate of 300 rpm for 40 min to prepare 5000 mg/L liquor and diluted by 1200 mg/L polymer solution in the liquor.

Fuzzy-ball fluid: 1.3% by mass of fuzzy-ball coating, 0.6% by mass of fuzzy-ball floss, 0.8% by mass of fuzzy-ball core, and 0.4% by mass of fuzzy-ball membrane were blended with simulated formation water for 40 min under a shearing rate of 8000 rpm and cooled to room temperature.

Preparation of cores: ① Saturated simulated formation water. Cores were put into a core saturation device. Cores were

https://doi.org/10.1021/acsomega.1c05427
ACS Omega 2021, 6, 34035−34043

vacuumed for 6 h when the vacuum degree was above 0.098 MPa and then were pressurized for 6 h when the pressure was 5 MPa. ② Saturated oil. Oil was injected into cores for 2 h at a temperature of 57 °C, a confining pressure of 5 MPa, and an injection rate of 1.0 mL/min. Then, cores were aged for 48 h at 57 °C. After preparation, PV was calculated using eq 3, and oil saturation was calculated using eq 4.

$$V_P = \frac{m_{aft} - m_{bef}}{\rho} \quad (3)$$

$$S_O = \frac{V_O}{V_P} \times 100\% \quad (4)$$

where m_{bef} and m_{aft} are mass of cores before and after saturating formation water, respectively; ρ is the density of simulated formation water; V_O and V_P are volumes of oil and pore volume, respectively; and S_O is oil saturation. The pore volume, oil saturation of artificial sandstone cores, and other useful information are listed in Table 1.

Table 1. Basic Information of Artificial Sandstone Cores

experimental type	core no.	pore volume (mL)	porosity (%)	volume of oil (mL)	oil saturation (%)
seepage behavior experiments	200-1	123	20.25	102	82.93
	600-1	128	21.07	103	80.47
	1200-1	126	20.74	104	82.54
	5000-1	130	21.40	106	81.54
parallel core displacement experiments	200-2	120	19.75	98	81.67
	600-2	124	20.41	102	82.26
	200-3	121	19.92	99	81.82
	1200-2	126	20.74	103	81.75
	200-4	121	19.92	100	82.64
	5000-2	125	20.58	101	80.80

5.3. Seepage Behavior Experiments. As seen in Figure 12, the seepage behavior experiment system primarily consists of injection pumps, a core holder, and a confining pressure control system. To obtain the reservoir temperature (57 °C), the core holder, brine cylinder, and fuzzy-ball fluid cylinder were placed in a thermotank. Experiments on seepage behavior were conducted in the following steps: To begin, a core with a permeability of 200 mD (or 600, 1200, or 5000 mD) was placed in the core holder for 2 h to guarantee that the core temperature is 57 °C. Then, at a flow rate of 1.5 mL/min, simulated formation water was injected into the core, and the experiment was ended when the inlet pressure stabilized. Third, fuzzy-ball fluid was injected into the core at a flow rate of 1.5 mL/min, and the experiment was not halted until 0.6 PV fuzzy-ball fluid was injected; fourth, simulated formation water was injected into the core at a flow rate of 1.5 mL/min for 0.6 PV, and the experiment was then stopped. The inlet pressure was recorded every 5 min during all injection processes, and all inlet pressures were measured to calculate the maximum resistance coefficient (F_{MR}) and maximum residual resistance coefficient (F_{MRR}).

5.4. Parallel Core Displacement Experiments. The formation heterogeneity was simulated by paralleling cores with varying permeabilities. The following procedures were used to conduct the experiments: to begin, simulated formation water was pumped into cores at a rate of 1.5 mL/min, a confining pressure of 5 MPa, and a temperature of 57 °C until the instantaneous water content of the high permeability core exceeded 80%. Every 5 min, the intake pressure, water volume, and total liquid volume were measured during the trials. 0.6 PV fuzzy-ball fluid was then injected. Following that, 1.5 mL/min of 0.6 PV simulated formation water was injected into cores. As illustrated in Figure 13, the experimental system is composed mostly of injection pumps, core holders, and a confining pressure control system. To attain the reservoir temperature (57 °C), a thermotank was filled with core holders, brine cylinders, polymer cylinders, and fuzzy-ball fluid cylinders.

5.5. Microcharacterization Experiment. *5.5.1. Characterization of the Microstructure of the Fuzzy Ball.* The optical microstructure device and cryo-electron microscopy were applied to characterize the microstructure of the fuzzy ball at room temperature.

(1) Characterization of the optical microstructure. A small bit of the fuzzy-ball fluid was sucked with a glue-head dropper and then dropped and spread on the glass slide. Then, the glass slide was placed on the microscope's stage for observation. The optical microstructure device has a magnification range of 40 to 400 times.

(2) Cryo-electron microscopy characterization. A certain volume of fuzzy-ball fluid was poured into the watch glass, and then, the watch glass was put in liquid nitrogen for freezing. After the freezing is complete, the watch glass was taken out and a knife was used to cut a

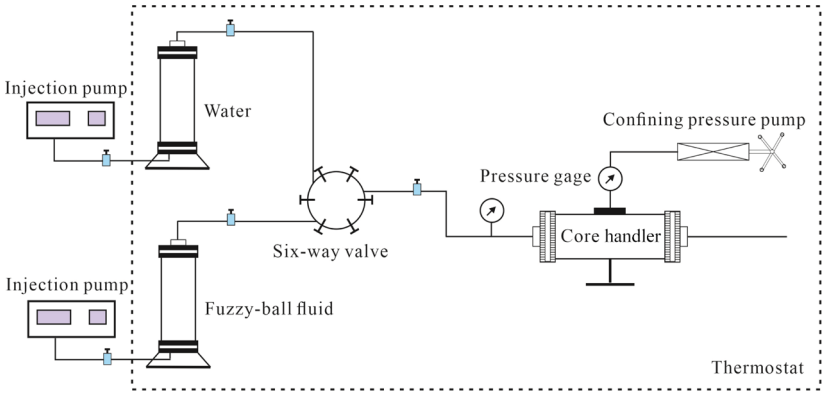

Figure 12. Seepage behavior experiment process diagram.

https://doi.org/10.1021/acsomega.1c05427
ACS Omega 2021, 6, 34035−34043

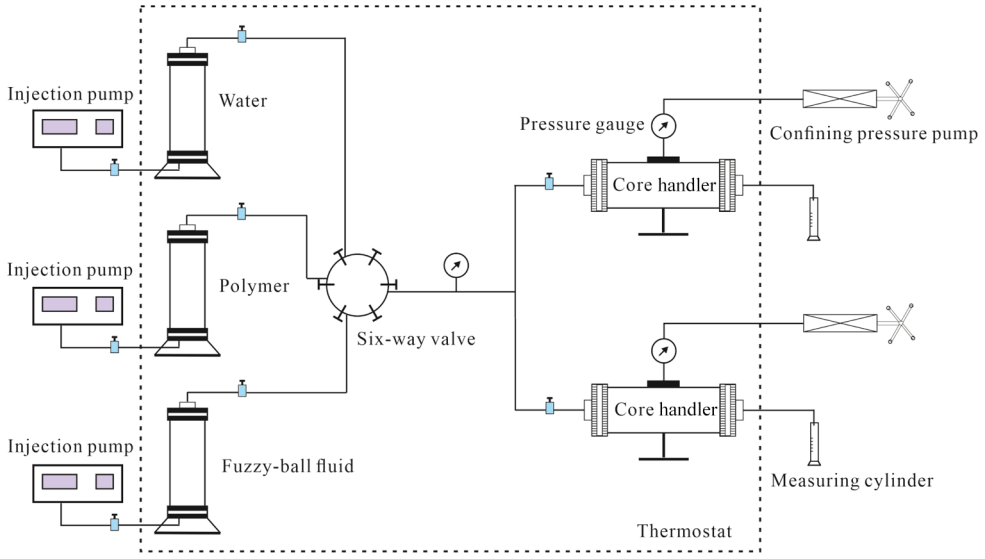

Figure 13. Injection timing experiment process diagram.

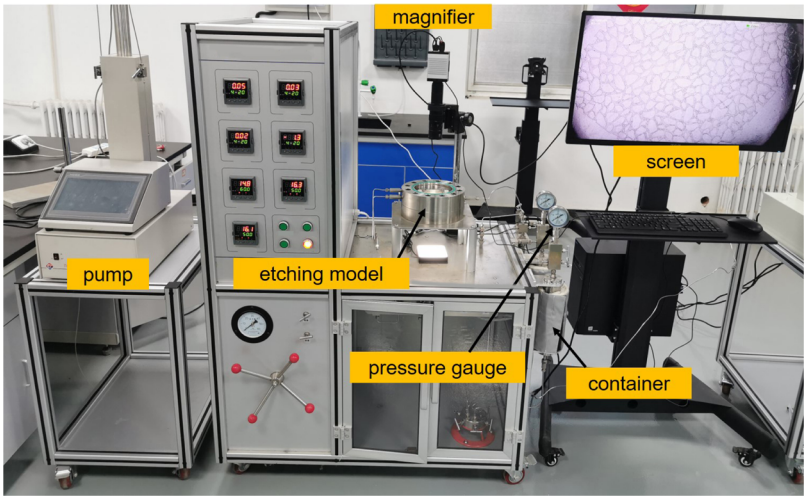

Figure 14. Microscopic glass etching model observation device.

thin slice of the frozen fuzzy-ball fluid. Finally, it was observed with an electron microscope. The magnification of cryo-electron microscopy is 2500 times.

5.5.2. Measurements of the Contact Angle. At room temperature, contact angle measurements were taken with a JC2000D4 Contact Angle Measuring Instrument. The core was cut into thin slices, which were then used to measure contact angles. After the measurement is complete, the "angle method" was used to calculate the contact angle of the fuzzy-ball fluid on the core surface.

5.5.3. Microscopic Glass Etching Model Experiment. A microscopic glass etching model observation device, as shown in Figure 14, was used to characterize the sealing mechanism of the fuzzy-ball fluid. The experiment was conducted at room temperature. The flow rate is 0.001 mL/min during the experiment, and the confining pressure is maintained 2 MPa higher than the inlet pressure. The computer can record and save experimental data automatically.

5.5.4. Microscopic Glass Etching Model Experiment. The pore size distribution of cores was measured using a Micromeritics Auto Pore IV 9500. A small piece of core cuttings was removed and the cuttings were ground into powder. The powder with a particle size of less than 200 mesh is then selected using standard sieving. Then, the powder was put into a Micromeritics Auto Pore IV 9500 to determine the pore size distribution of the cores. The pressure range for testing is 0−200 MPa. All operations are carried out at room temperature.

AUTHOR INFORMATION

Corresponding Authors

Chao Wang − *Institute of Petroleum Engineering, China University of Petroleum (Beijing), Beijing 102249, China;* orcid.org/0000-0002-8684-1024; Email: chaowang9999@outlook.com

Lihui Zheng − *Institute of Petroleum Engineering, China University of Petroleum (Beijing), Beijing 102249, China;* Email: 2598760275@qq.com

Authors

Hao Liu − *Institute of Petroleum Engineering, China University of Petroleum (Beijing), Beijing 102249, China*

https://doi.org/10.1021/acsomega.1c05427
ACS Omega 2021, 6, 34035−34043

Xiangchun Wang − *Institute of Petroleum Engineering, China University of Petroleum (Beijing), Beijing 102249, China*

Complete contact information is available at: https://pubs.acs.org/10.1021/acsomega.1c05427

Notes

The authors declare no competing financial interest.

■ ACKNOWLEDGMENTS

The study was supported by the Technology Major Projects of China (no. 2016ZX05025). A microscopic glass etching model observation device was provided by Jiangsu Tuochuang Scientific Research Instrument Co., Ltd.

■ REFERENCES

(1) Jia, H.; Lian, P.; Leng, X.; Han, Y.; Wang, Q.; Jia, K.; Niu, X.; Guo, M.; Yan, H.; Lv, K. Mechanism studies on the application of the mixed cationic/anionic surfactant systems to enhance oil recovery. *Fuel* **2019**, *258*, 116156.

(2) Rellegadla, S.; Prajapat, G.; Agrawal, A. Polymers for enhanced oil recovery: fundamentals and selection criteria. *Appl. Microbiol. Biotechnol.* **2017**, *101*, 4387−4402.

(3) Xin, X.; Yu, G.; Chen, Z.; Wu, K.; Dong, X.; Zhu, Z. Effect of polymer degradation on polymer flooding in heterogeneous reservoirs. *Polymers* **2018**, *10*, 857.

(4) Liu, P.; Mu, Z.; Wang, C.; Wang, Y. Experimental study of rheological properties and oil displacement efficiency in oilfields for a synthetic hydrophobically modified polymer. *Sci. Rep.* **2017**, *7*, 8791.

(5) Yan, L.; Ding, W. Flooding performance evaluation of alkyl aryl sulfonate in various alkaline environments. *PLoS One* **2019**, *14*, No. e0219627.

(6) Druetta, P.; Picchioni, F. Surfactant−Polymer Flooding: Influence of the Injection Scheme. *Energy Fuels* **2018**, *32*, 12231−12246.

(7) Huang, B.; Li, X.; Zhang, W.; Fu, C.; Wang, Y.; Fu, S. Study on Demulsification - Flocculation Mechanism of Oil - Water Emulsion in Produced Water from Alkali/Surfactant/Polymer Flooding. *Polymers* **2019**, *11*, 395.

(8) Wang, Z.; Hu, R.; Ren, G.; Li, G.; Liu, S.; Xu, Z.; Sun, D. Polyetheramine as an alternative alkali for alkali/surfactant/polymer flooding. *Colloids Surf., A* **2019**, *581*, 123820.

(9) Dabiri, A.; Honarvar, B. Synergic Impacts of Two Non-ionic Natural Surfactants and Low Salinity Water on Interfacial Tension Reduction, Wettability Alteration and Oil Recovery: Experimental Study on Oil Wet Carbonate Core Samples. *Nat. Resour. Res.* **2020**, *29*, 4003−4016.

(10) Chen, F.; Gu, J.; Jiang, H.; Yao, X.; Li, Y. Laboratory evaluation and numerical simulation of the alkali - surfactant - polymer synergistic mechanism in chemical flooding. *RSC Adv.* **2018**, *8*, 26476−26487.

(11) Wang, D. M.; Cheng, J. C.; Wu, J. Z.; Wang, G. Application of polymer flooding technology in Daqing oilfield. *Acta Pet. Sin.* **2005**, *26*, 74−78.

(12) Sun, H. Q. Practice and understanding on tertiary recovery in Shengli oilfield. *Pet. Explor. Dev.* **2006**, *33*, 262−266.

(13) Guo, Y. H.; Shu, D.; Liu, Z. J.; Li, Y.; Jiang, W. J.; Li, P. Y.; Yang, Y. L. Analysis and application on ultrahigh molecular weight polymer flooding in Gucheng oilfield. *Oilfield Chem.* **2019**, *36*, 325−330.

(14) Shi, L. T.; Zhu, S. J.; Ye, Z. B.; Xue, X. S.; Liu, C. L.; Lan, X. T. Effect of microscopic aggregation behavior on polymer shear resistance. *J. Appl. Polym. Sci.* **2019**, *137*, 48670.

(15) Yang, C. C.; Yue, X. A.; Zhou, D. Y.; He, J.; Zhao, J.; Zhou, J. L.; Li, C. Y. Performance evaluation of polymer microsphere with high temperature resistance and high salinity tolerance. *Oilfield Chem.* **2016**, *33*, 254−260.

(16) Lai, N. J.; Zhang, X.; Ye, Z. B.; Li, X.; Li, Z. H.; Wen, Y. P.; Zhang, Y. Laboratory study of an anti-temperature and salt-resistance surfactant-polymer binary combinational flooding as EOR chemical. *J. Appl. Polym. Sci.* **2014**, *131*, 596−602.

(17) Gao, Q.; Zhong, C. R.; Han, P. H.; Cao, R. B. Characteristics of Preferential Flow Paths in Reservoirs After Polymer Flooding and an Adaptive Compound Flooding Method. *Chem. Technol. Fuels Oils* **2021**, *57*, 368−375.

(18) Deng, X. J.; Zhang, X. L.; Zhu, J.; An, Y. M. Pattern of preferential reservoir water flow passage and discriminator analysis. *Oil Drill. Prod. Technol.* **2014**, *36*, 69−74.

(19) Wang, D.; Seright, R. S.; Shao, Z.; Wang, J. Key aspects of project design for polymer flooding. *Proceedings of the 2007 SPE Annual Technical Conference and Exhibition*; Society of Petroleum Engineers: Richardson, TX, 2007, pp 1117−1124.

(20) Gong, H.; Zhang, H.; Xu, L.; Li, K.; Yu, L.; San, Q.; Li, Y.; Dong, M. The synergistic effect of branched-preformed particle gel and hydrolyzed polyacrylamide on further-enhanced oil recovery after polymer flooding. *Energy Fuels* **2017**, *31*, 7904−7910.

(21) Zheng, L.; Kong, L.; Cao, Y.; Wang, H.; Han, Z.; He, X. The mechanism for fuzzy-ball working fluids for controlling & killing lost circulation. *Chin. Sci. Bull.* **2010**, *55*, 4074.

(22) Yan, X. J. *Research on the Development and Practice of School-Based Curriculum of Biology Life-Oriented Teaching in Pingbian NO.3 Middle School*; Yunnan Normal University: Yunnan, 2019; pp 110.

(23) Liu, B.; Xue, Z. L.; Zhang, K.; Wang, L. N.; Zhong, S. P. Application to fuzzy ball drilling fluid technology of coalbed methane U shaped horizontal connected wells. *Coal Sci. Technol.* **2015**, *43*, 105−109.

(24) Zheng, L. H.; Cao, Y.; Han, Z. X. Novel low-density drilling fluid containing fuzzy ball structure. *Acta Pet. Sin.* **2010**, *31*, 490−493.

(25) Wang, S.; Cao, Y. F.; Jiang, W. J.; Zhou, D. Z.; Jin, Y.; Liu, Y. Workover technology using fuzzy-ball temporary plugging fluid in Bohai Oilfield. *Oil Drill. Prod. Technol.* **2015**, *37*, 114−117.

(26) Zhu, L. G.; Huang, B.; Chen, W. Y.; Sun, L.; Liang, D.; Jiang, M. Q.; Feng, L. J. Fuzzy-ball fluid for stabilizing oil production and water control in formations with high-salinity water. *Oil Drill. Prod. Technol.* **2016**, *38*, 216−220.

(27) Zheng, L. H.; Cui, J. B.; Nie, S. S.; Liu, B.; Fu, Y. W.; Li, Z. Y. Temporary Plugging Diverting Test with Fuzzy Ball Fluids in Non-Water Producing Coal Beds in Re-fracturing Well Zheng-X. *Drill. Fluid Completion Fluid* **2016**, *33*, 103−108.

(28) Zheng, L. H.; Weng, D. W. Study on Repeating Fracturing while Causing No Damage to Original Fractures. *Drill. Fluid Completion Fluid* **2015**, *32*, 76−78.

(29) Wei, P.; Zheng, L.; Yang, M.; Wang, C.; Chang, Q.; Zhang, W. Fuzzy-ball fluid self-selective profile control for enhanced oil recovery in heterogeneous reservoirs: The techniques and the mechanisms. *Fuel* **2020**, *275*, 117959.

(30) Gao, Q.; Zhong, C. R.; Han, P. H.; Cao, R. B.; Jiang, G. Q. Synergistic Effect of Alkali - Surfactant - Polymer and Preformed Particle Gel on Profile Control after Polymer Flooding in Heterogeneous Reservoirs. *Energy Fuels* **2020**, *34*, 15957.

(31) Wang, C.; Zhong, L.; Liu, Y.; Han, Y.; Zhao, P.; Yuan, Y.; Han, X. Characteristics of Weak-Gel Flooding and Its Application in LD10-1 Oilfield. *ACS Omega* **2020**, *5*, 24935−24945.